Cosmic Ray Anisotropy Workshop 2013 (CRA2013) IOP Publishing
Journal of Physics: Conference Series **531** (2014) 012010 doi:10.1088/1742-6596/531/1/012010

Anisotropies in TeV Cosmic Rays Related to the IBEX Ribbon

N. A. Schwadron[1,2], F. C. Adams[3], E. Christian[4], P. Desiati[5], P. Frisch[6], H. O. Funsten[7], J. R. Jokipii[8], D. J. McComas[2,9], E. Moebius[1], G. Zank[10]

[1] University of New Hampshire, Durham, NH, 03824
[2] Southwest Research Institute, San Antonio, TX 78228, USA
[3] University of Michigan, Ann Arbor, MI, 48109
[4] Goddard Spaceflight Institute
[5] IceCube Research Center and Astronomy Department, University of Wisconsin, Madison, WI 53706
[6] University of Chicago, Department of Astronomy and Astrophysics, Chicago, IL 60637
[7] Los Alamos National Laboratory, Los Alamos, NM, 87545
[8] University of Arizona
[9] University of Texas, San Antonio, TX 78228, USA
[10] University of Alabama Huntsville

E-mail: n.schwadron@unh.edu

Abstract. The Interstellar Boundary Explorer (IBEX) observes enhanced Energetic Neutral Atoms (ENAs) emission in the keV energy range from a narrow ($\sim$20° wide) "ribbon" in the sky that appears to be centered on the direction of the local interstellar (LIS) magnetic field. The Milagro collaboration, the Asγ collaboration and the IceCube observatory have recently made global maps of cosmic ray fluxes in the TeV energy range, revealing anisotropic structures ordered in part by the local interstellar magnetic field and the interstellar flow. This paper following from a recent publication in *Science* makes the link between these disparate observations by developing a simple model of the magnetic structure surrounding the heliosphere in the Local Interstellar Medium (LISM) that is consistent with both IBEX ENA fluxes and TeV cosmic ray anisotropies. The model also employs the revised velocity direction of the LIC derived from neutral He observations by IBEX. By modeling the propagation of cosmic rays through this magnetic field structure, we specifically show that (1) the large-scale TeV anisotropy provides a roughly consistent orientation for the local interstellar magnetic field at the center of the IBEX Ribbon and corroborates the ~ 3 μG magnitude of the local interstellar magnetic field derived from IBEX observations of the global heliosphere; (2) and small-scale structures in cosmic rays (over $< 30°$ angular scales) are influenced by the interstellar field interaction with the heliosphere at energies < 10 TeV. Thus, we provide a link between IBEX ENA observations, IBEX neutral observations of interstellar He, and TeV cosmic ray anisotropies, which are strongly influenced by the interactions between the local interstellar magnetic field, the flow of the local interstellar plasma, and the global heliosphere.

1. Introduction

The Interstellar Boundary Explorer Mission (IBEX) was launched October 19, 2008, with the objective to discover the global interaction between the solar wind and the local interstellar

medium [1]. IBEX measures Energetic Neutral Atoms (ENAs) created predominantly from charge-exchange between neutral interstellar hydrogen and plasma protons in the solar wind and interstellar medium [1; 2]. First results from IBEX include global maps of the heliosphere in ENAs [3–6] and the first measurements of low energy interstellar oxygen, helium and hydrogen atoms [7]. Higher energy maps from INCA were also revealed [8]. The IBEX and INCA sky maps showed striking differences between observations and predictions from models [6].

The IBEX maps revealed the existence of a narrow ribbon ($\sim 20^\circ$ wide) of elevated ENA emissions [3–5] that forms a circular structure centered on (RA, DEC) $\sim$ (48.5°$\pm$1.5, -21.2°$\pm$1.6), which is likely near the local interstellar (LISM) magnetic field direction [6].

This paper discusses another observational signature of this LISM magnetic field in TeV cosmic ray anistropies [9]. Figure 1 shows the cosmic ray gyroradius for a typical field strength in the heliosheath (1 μG, blue) and LISM (3 μG, red). In the energy range from 0.5 to 10 TeV, cosmic rays with gyroradii of 100's of AU probe the scales in the LISM that are larger than the heliosphere. Recall that the deformation of the LIsMF also extends to 100's of AU. Therefore, it is precisely in the $\sim$ 0.5-10 TeV energy range where cosmic rays may probe the same large scale LIsMF structures apparently manifested in the IBEX Ribbon.

2. Cosmic Ray Anisotropy Observations

The arrival direction distribution of cosmic rays from tens of GeV to tens of TeV is found to have an asymmetry which is not compatible with the convection anisotropy expected by the motion of the solar system through the galactic medium [10; 11]. A broad relative excess is observed between equatorial right ascension $\alpha \approx 18$ hr and $\alpha \approx 8$ hr, with an amplitude of $10^{-4} - 10^{-3}$. The global structure of the anisotropy depends on the cosmic ray energy, but is found to change weakly in the energy range from about 1 TeV to a few tens of TeV. Fig. 2 (panel A) shows the map in equatorial coordinates of relative intensity in the cosmic ray arrival direction, as observed by Tibet ASγ in the northern equatorial hemisphere at a median energy of about 5 TeV [12], and by the IceCube Observatory in the southern equatorial hemisphere at a median energy of about 20 TeV [13]. In each declination band of about 5° the relative intensity represents the modulation of the counting rate with respect to the mean rate in that declination. The two observations reported in the figure correspond to different median energies, although the observations span a wide energy range to collect the large event sample needed for the determination of the small anisotropy amplitude. In particular IceCube reported that 68% of the data sample with median energy of about 20 TeV is between 4 TeV and 63 TeV [14]. Assuming an equivalent resolution for the Tibet ASγ, it turns out that the two data samples are significantly overlapped in cosmic ray energy, and therefore they can be directly compared. In Fig. 2 (panel A) it appears that the relative excess in arrival direction is oriented toward the region of the sky that comprises the downstream direction of the interstellar wind and the downfield direction for the LIsMF.

In order to accentuate the small scale features that appear on the global anisotropy sky map, the Milagro Collaboration subtracted a 30°-averaged sky map from that of the global anisotropy [see 15, for details]. The residual map highlights all the fine structures with characteristic angular scales that are smaller than 30°. A similar analysis was performed by the IceCube Observatory, where the averaging procedure was performed within 60°, meaning that only features smaller than such an angular scale are highlighted. Fig. 2 (panel B) shows the corresponding map in equatorial coordinates of the statistical significance with respect to the averaged maps and with a 10° smoothing. The northern hemisphere shows the result from Milagro at a mean energy of $\sim$1 TeV and the southern hemisphere shows the IceCube observations at a median energy of $\sim$ 20 TeV. Once again, although the characteristic energies of the two observations are different, the energy ranges of the observations significantly overlap. Some interesting visual correlation between the two halves of the sky arise.

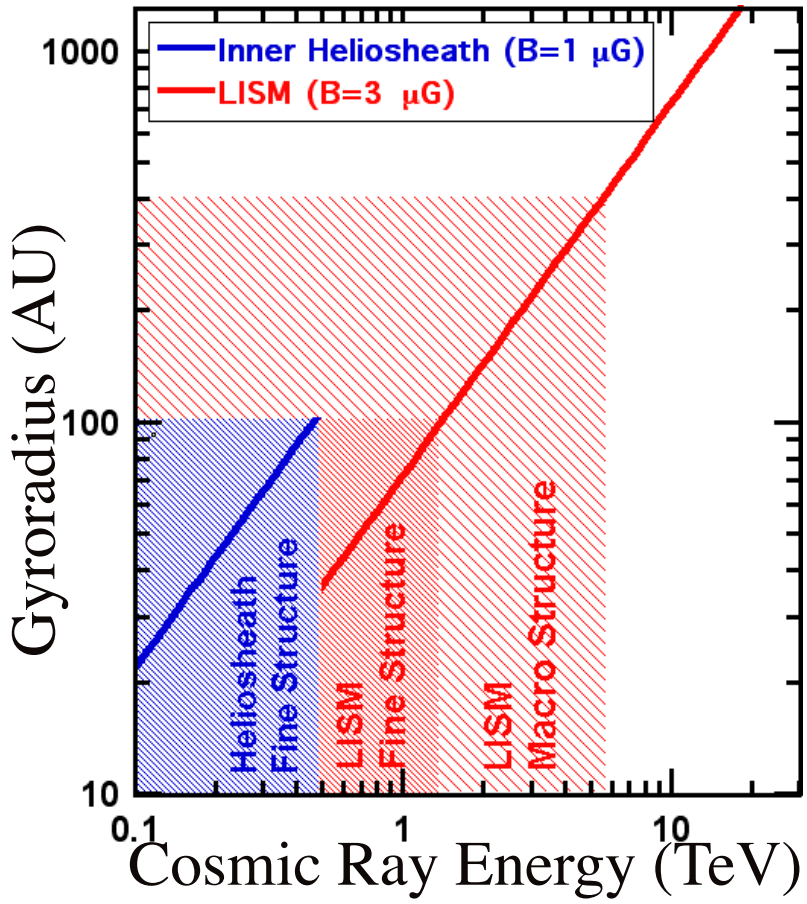

Figure 1. The gyroradius of cosmic rays in the heliosheath (1 μG, blue) and LISM (3 μG, red) probe increasingly large structures with increasing energy. Cosmic rays probe the heliosheath structure in the $\sim$ 0.1-0.5 TeV energy range, LISM fine structure $<$ 100 AU in the $0.5-1.5$ TeV energy and LISM macrostructure including the distortion of the LISM field around the heliosphere of 100's of AU for energies between $\sim 1.5-10$ TeV. It is over this energy TeV energy range where cosmic rays probe the same magnetic structures from the LISM that likely produce the IBEX Ribbon. [From 9].

In both sky maps, the localized excess of cosmic ray flux observed at equatorial coordinates $(\alpha, \delta) \approx$ (21 hr, +32°) is due to gamma rays from the Cygnus region to which both Tibet ASγ and Milagro are sensitive. In the southern hemisphere, the most significant localized excess and deficit regions at $(\alpha, \delta) \approx$ (7 hr, -45°) and $(\alpha, \delta) \approx$ (15 hr, -45°), respectively, correspond to the center of the global anisotropy regions, meaning that some of the large scale structure influences features in the residual sky map. The Milagro observation of a localized fractional excess in the direction of the heliotail does not appear to have a correspondance in the southern sky. On the other hand, the filamentary feature at right ascension $\alpha \approx$ 8-10 hr, appears to continue throughout the South in a quasi-circular pattern, even though here its statistical significance is not as high. Given the width of the energy response functions, it is possible that cosmic rays contributing to different localized regions have different characteristic energy. More observations are needed to refine these maps.

Fig. 2 (panel C) shows the IBEX Ribbon observed at 1.1 keV [3–6] in J2000 coordinates. We include labels for the upwind and downwind directions [16], the Voyager 1 (V1) and Voyager 2

(V2) directions and the upfield and downfield directions associated with the unperturbed LISM magnetic field. The black line shows the magnetic equator of the external LIsMF in the direction of the IBEX Ribbon center. The shift of the Ribbon to the inside of the LIsMF magnetic equator is likely due to flaring of the field on the noseward side of the heliosphere [6]. The global structure in all three panels is ordered about the LIsMF magnetic equator, which reinforces the concept that the LIsMF influences both TeV cosmic rays and the ENA fluxes observed by IBEX.

3. Local Interstellar Structure

The heliosphere interacts with the local interstellar flow that originated from the center of Loop I. Typical temperatures are $\sim 3000 - 13000$ K and proton densities $\sim 0.05 - 0.1$ cm^{-3} [18]. Deviations of the velocities of individual clouds from a rigid-body flow indicate that the flow is decelerating [19]. A decelerating flow sets the conditions for collisions between the local clouds. The Sun is inside of the LIC and no more than 0.1 pc away from the LIC edge in the direction of the galactic center hemisphere [20; 21]. In the direction of the anticenter hemisphere, the closest cloud to the LIC is the 'Blue Cloud' [BC, 22; 23]. Linsky *et al.* [24] show that the conditions for colliding clouds exist within ~ 10 pc, with relative velocities between overlapping clouds of up to 50 km s^{-1} (Figure 3). Among the closest of possible collisions would be a collision between the LIC and BC.

Cloud collisions in this region are supported by observations of short-timescale scintillation towards two compact radio sources, PKS 0405-385 and PSR J0437-47, which are located behind the BC [25]. Models of the timescales and frequency dependence of the scintillation show that the scattering screens, consisting of partially ionized gas such as the LIC, are within ~ 10 pc. Towards PSR J0437-47, the local turbulence occurs over spatial scales of ~ 0.02 AU [26]. PKS 0405-385 and PSR J0437-47 are located within 29° of the downfield direction.

The decelerating flow of local interstellar clouds past the Sun appears to be ordered by an evolved superbubble associated with Loop I [18]. An interstellar magnetic field interacting with the compressed, perhaps inhomogeneous, shell provides a natural explanation for inhomogeneities in the LIsMF. Figure 4 shows the flow of local clouds through the LSR for a meridianal cut through the galactic plane where the Z-direction is directed toward galactic north and the X-direction is toward galactic center. Measurements of interstellar He I inside of the heliosphere provide the LIC velocity [27; 28], while velocities for 15 local clouds have been determined with the triangulation of the radial velocity component towards different stars behind the clouds [25]. The Loop I superbubble shell is represented by the thick arc, which is based on the S1 shell of Wolleben [29] that is centered ≈ 78 pc away at galactic coordinates of L,B$\approx$346°,3° [29].

Measurements of He I inside of the heliosphere provide the LIC velocity [27; 28]. Pressure equilibrium between the gas and magnetic field in the LIC give a LIC magnetic field strength of ~ 2.7 μG, which is comparable to the ~ 3 μG field strength obtained from the globally distributed ENA fluxes [30].

4. Imprint of the heliosphere on the global anisotropy in TeV cosmic rays

Schwadron *et al.* [9] utilized the observations of IBEX to estimate the direction of the magnetic field in the LISM. Knowing in addition the flow velocity of the LISM based on neutral He measurements, we developed model estimates for the global anisotropy of TeV cosmic rays in the LISM associated with modulation by the local interstellar flow. The flow configuration of the LISM has a flow velocity almost perpendicular to the local interstellar magnetic field and consistent with the outward expansion of plasma from the Loop I S1 superbubble (Fig. 5). The model also includes the propagation effects associated with deformation of the local interstellar magnetic field about the heliosphere. The resulting global anisotropy map in TeV cosmic rays is shown in Fig. 6. The full calculation is detailed by Schwadron et al. [9]. The main free parameter

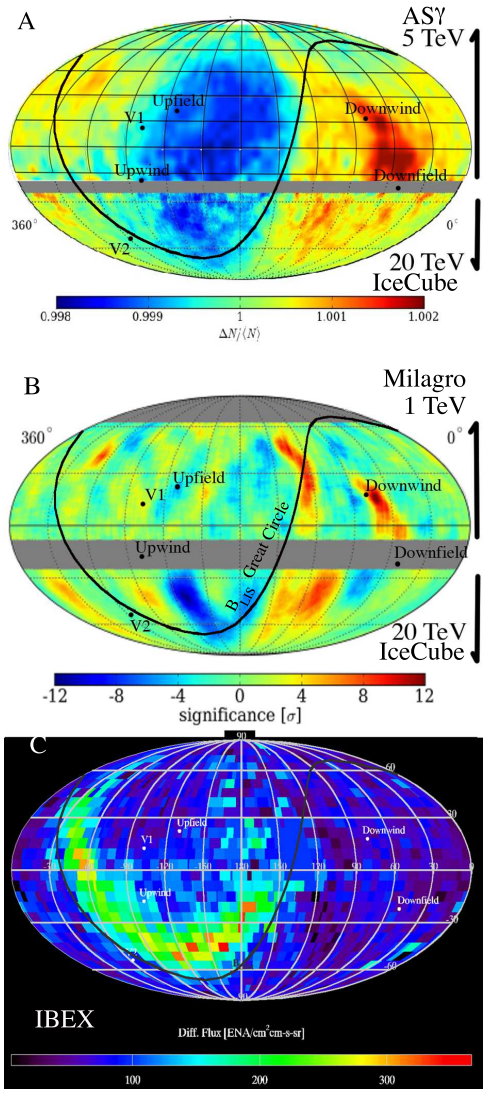

Figure 2. *Panel A*: relative intensity observed by Tibet Asγ collaboration at a median energy of $\sim$ 5 TeV [17] in the north and by IceCube in the south at a median energy of $\sim$ 20 TeV [13]. Both portions of the maps are smoothed with 3°-5°. *Panel B*: significance map that smoothes (over 30°-60°) and filters out the large scale anisotropy to reveal only the small scale anisotropy. The northern hemisphere is from the Milagro project, centered on $\sim$ 1 TeV median energy [15]. The southern hemisphere is the map from the IceCube collaboration at $\sim$20 TeV median energy [13]. *Panel C*: The IBEX Ribbon observed at $\sim$ 1.1 keV [3–6] in J2000 coordinates and the TeV Milagro/Ice Cube data. We include labels for the upwind and downwind directions [16], the Voyager 1 (V1) and Voyager 2 (V2) directions and the upfield and downfield directions associated with the unperturbed LIsMF. The TeV cosmic ray data appears to be ordered by the LISM magnetic equator. These plots are in equatorial coordinates with $\alpha = 0$ hr at the right, and increasing towards the left.

in these estimates of the global TeV anisotropy is the level of perpedindicular diffusion for which we use typical parameters of the ISM that $\kappa_\perp/\kappa_\parallel \sim 0.003$ [32].

Supernova remants (SNR) also contribute to the anisotropy, at least in localized regions. While the direction of LISM magnetic field found by IBEX must play a significant role in

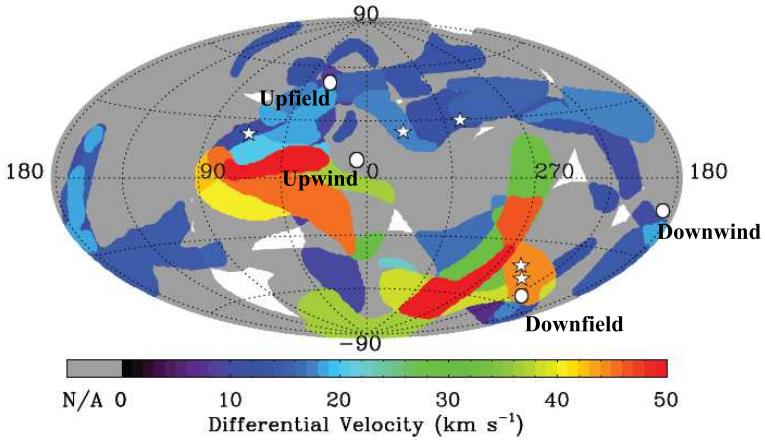

Figure 3. Zones of LISM cloud interaction with superposed upwind, downwind, upfield and downfield directions. Colored regions show the directions in which multiple LISM clouds are detected along the line of sight. The white regions indicate where no LISM cloud is detected, and gray regions where only a single cloud is detected. The color coding signifies the maximum magnitude of the differential velocity between clouds along the same line of sight. Five scintillation sight lines are shown here by star symbols. This plot is in galactic coordinates, and centered on the galactic center with longitude increasing towards the left. [Based on 24].

ordering the cosmic ray anisotropy map, the sign of the dipolar anisotropy component could either align with or oppose the component that arises from local interstellar modulation. Further, the magnitude of the dipolar component of the cosmic ray anisotropy is poorly constrained by observations.

5. Conclusions

The comparison shown in Figure 5 confirms the direction of the LISM magnetic field from the center of the IBEX ribbon. The result is somewhat surprising since the LISM magnetic field from the IBEX ribbon is determined in a very local interstellar environment, within 100's of AU from the heliosphere. Turbulence in the LISM might be expected to destroy signatures of the direction inferred from IBEX over 1-10 pc correlation scales. Such effects would obscure any relationship between global TeV cosmic ray anistropies and the IBEX ribbon. The fact that a relationship is observed suggests that the LISM magnetic field remains relatively coherent over scales of at least 1-10 pc. This in turn suggests that our heliosphere is currently moving through a magnetically ordered portion of the LISM. This reinforces the concept that the LISM magnetic field has sufficient pressure to play a significant role in LISM dynamics.

Thus, we have shown that TeV cosmic rays provide independent confirmation of the direction of the LISM magnetic field inferred from the center of the IBEX ribbon. The correlation is remarkable given that these independent observations are taken over vastly different energy ranges. IBEX measures energetic neutral atoms at thousands of eV and TeV anisotropy maps are formed from particles at higher energies by ten orders of magnitude. Our increasing understanding of the local interstellar environment is particularly important considering that the Voyager 1 spacecraft is now entering interstellar space.

5.1. Acknowledgments

We are deeply indebted to all of the outstanding people who have made the IBEX mission possible and have contributed to the Asγ, IceCube and Milagro projects. This work was carried

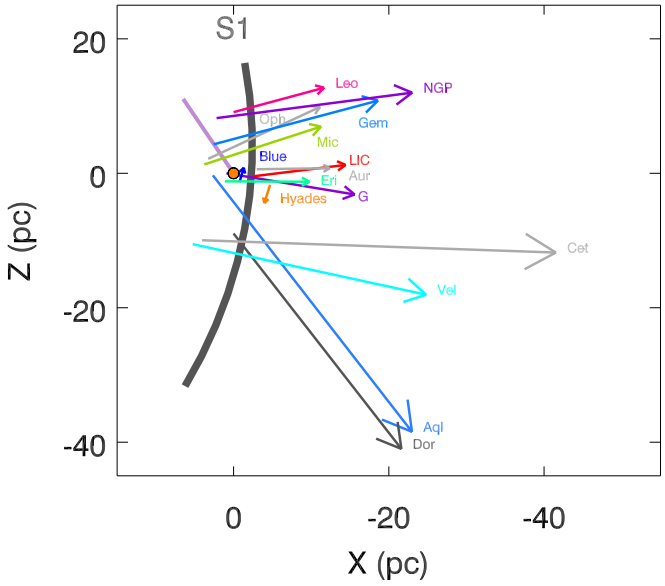

Figure 4. The arrows show the velocities of local interstellar clouds through the LSR in the X-Z meridian plane, where the X-axis is directed towards the galactic center and the Z-axis is directed towards the galactic north pole [based on heliocentric velocities in 25]. The LSR velocities are calculated using the solar apex motion [from 31]. The arrow origin is located at the cloud-center and the distance of the nearest star (that is not the Sun) in the cloud. Arrows are labeled with cloud names. The thick gray arc shows the location of the Loop I S1 superbubble, based on a thin shell with radius of 78 pc that is centered at galactic coordinates of L,B=346°,3° [29]. The purple line gives the direction of the LIsMF [4] and the orange dot shows the solar location.

out as a part of the IBEX project, with support from NASAs Explorer Program.

References

[1] McComas D J, Allegrini F, Bochsler P, Bzowski M, Collier M, Fahr H, Fichtner H, Frisch P, Funsten H O, Fuselier S A, Gloeckler G, Gruntman M, Izmodenov V, Knappenberger P, Lee M, Livi S, Mitchell D, Möbius E, Moore T, Pope S, Reisenfeld D, Roelof E, Scherrer J, Schwadron N, Tyler R, Wieser M, Witte M, Wurz P and Zank G 2009 *Space Sci. Rev.* **146** 11–33

[2] McComas D J, Funsten H O, Fuselier S A, Lewis W S, Möbius E and Schwadron N A 2011 *Geophys. Res. Lett.* **38** L18101

[3] McComas D J, Allegrini F, Bochsler P, Bzowski M, Christian E R, Crew G B, DeMajistre R, Fahr H, Fichtner H, Frisch P C, Funsten H O, Fuselier S A, Gloeckler G, Gruntman M, Heerikhuisen J, Izmodenov V, Janzen P, Knappenberger P, Krimigis S, Kucharek H, Lee M, Livadiotis G, Livi S, MacDowall R J, Mitchell D, Möbius E, Moore T, Pogorelov N V, Reisenfeld D, Roelof E, Saul L, Schwadron N A, Valek P W, Vanderspek R, Wurz P and Zank G P 2009 *Science* **326** 959–

[4] Funsten H O, Allegrini F, Crew G B, DeMajistre R, Frisch P C, Fuselier S A, Gruntman M, Janzen P, McComas D J, Möbius E, Randol B, Reisenfeld D B, Roelof E C and Schwadron N A 2009 *Science* **326** 964–

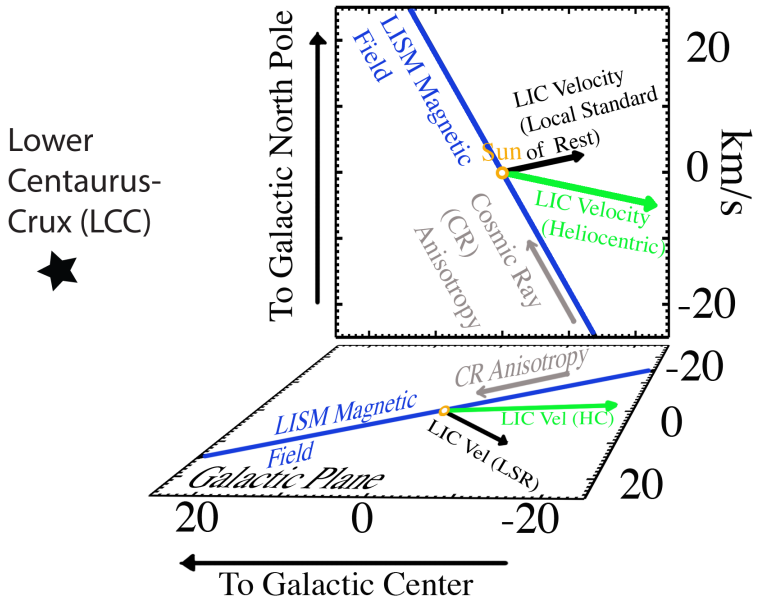

Figure 5. Directions and magnitudes of the LIC velocities inferred from IBEX in the heliocentric (HC; green vector) rest frame and the local standard of rest (LSR; black vector) in the galaxy. These vectors are shown in the galactic plane (lower plane) and the plane containing the galactic poles (upper plane) together with the magnetic field of the local interstellar medium (blue lines). The LIC velocity and magnetic field are a part of the Loop I superbubble roughly centered on the Lower Centaurus Crux (LCC). The cosmic ray anisotropy (grey vector) indicates average streaming of cosmic rays.

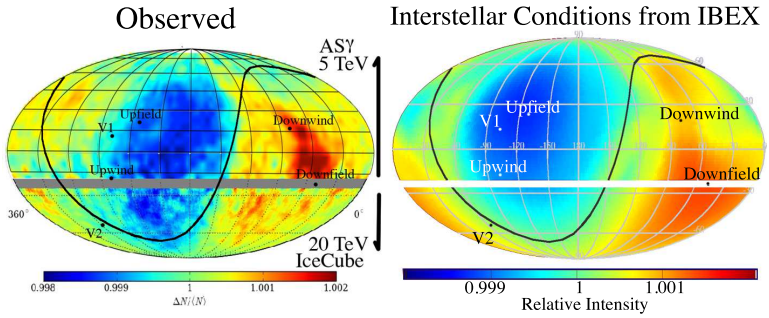

Figure 6. Comparison between observed (left) and modeled (right) cosmic ray intensities across the sky (J2000 coordinates). Black curves show the magnetic equator given a magnetic field direction derived from the center of the IBEX ribbon. (Left) The regions below 25° S latitude show the anisotropy map from IceCube with a median energy of 20 TeV and above 20° S latitude is the anisotropy map from AS-γ with 5 TeV median energy. (Right) The modeled map at 20 TeV is shown below 25° S latitude and at 5 TeV above 20° S latitude. [From 9].

[5] Fuselier S A, Allegrini F, Funsten H O, Ghielmetti A G, Heirtzler D, Kucharek H, Lennartsson O W, McComas D J, Möbius E, Moore T E, Petrinec S M, Saul L A, Scheer J A, Schwadron N and Wurz P 2009 *Science* **326** 962

[6] Schwadron N A, Bzowski M, Crew G B, Gruntman M, Fahr H, Fichtner H, Frisch P C, Funsten H O, Fuselier S, Heerikhuisen J, Izmodenov V, Kucharek H, Lee M, Livadiotis G, McComas D J, Moebius E, Moore T, Mukherjee J, Pogorelov N V, Prested C, Reisenfeld D, Roelof E and Zank G P 2009 *Science* **326** 966–

[7] Möbius E, Bochsler P, Bzowski M, Crew G B, Funsten H O, Fuselier S A, Ghielmetti A, Heirtzler D, Izmodenov V V, Kubiak M, Kucharek H, Lee M A, Leonard T, McComas D J, Petersen L, Saul L, Scheer J A, Schwadron N, Witte M and Wurz P 2009 *Science* **326** 969–

[8] Krimigis S M, Mitchell D G, Roelof E C, Hsieh K C and McComas D J 2009 *Science* **326** 971–

[9] Schwadron N A, Adams F C, Christian E R, Desiati P, Frisch P, Funsten H O, Jokipii J R, McComas D J, Moebius E and Zank G P 2014 *Science* **343** 988

[10] Compton A H and Getting I A 1935 *Physical Review* **47** 817–821

[11] Gleeson L J and Axford W I 1968 *Astrophys. J.* **154** 1011

[12] The Tibet Asγ Collaboration, Amenomori M, Bi X J, Chen D, Cui S W, Danzengluobu, Ding L K, Ding X H, Fan C, Feng C F, Feng Z, Feng Z Y, Gao X Y, Geng Q X, Guo H W, He H H, He M, Hibino K, Hotta N, Hu H, Hu H B, Huang J, Huang Q, Jia H Y, Kajino F, Kasahara K, Katayose Y, Kato C, Kawata K, Labaciren, Le G M, Li A F, Li J Y, Lou Y Q, Lu H, Lu S L, Meng X R, Mizutani K, Mu J, Munakata K, Nagai A, Nanjo H, Nishizawa M, Ohnishi M, Ohta I, Onuma H, Ouchi T, Ozawa S, Ren J R, Saito T, Saito T Y, Sakata M, Sako T K, Shibata M, Shiomi A, Shirai T, Sugimoto H, Takita M, Tan Y H, Tateyama N, Torii S, Tsuchiya H, Udo S, Wang B, Wang H, Wang X, Wang Y, Wang Y G, Wu H R, Xue L, Yamamoto Y, Yan C T, Yang X C, Yasue S, Ye Z H, Yu G C, Yuan A F, Yuda T, Zhang H M, Zhang J L, Zhang N J, Zhang X Y, Zhang Y, Yizhang, Zhaxisangzhu, Zhou X X and The Tibet ASγ Collaboration 2011 *Advances in Space Research* **47** 629–639

[13] Abbasi R, Abdou Y, Abu-Zayyad T, Adams J, Aguilar J A, Ahlers M, Andeen K, Auffenberg J, Bai X, Baker M and et al 2010 *Astrophys. J. Lett.* **718** L194–L198 (*Preprint* `1005.2960`)

[14] Abbasi R, Abdou Y, Abu-Zayyad T, Ackermann M, Adams J, Aguilar J A, Ahlers M, Allen M M, Altmann D, Andeen K and et al 2012 *Astrophys. J.* **746** 33 (*Preprint* `1109.1017`)

[15] Abdo A A, Allen B, Aune T, Berley D, Blaufuss E, Casanova S, Chen C, Dingus B L, Ellsworth R W, Fleysher L, Fleysher R, Gonzalez M M, Goodman J A, Hoffman C M, Hüntemeyer P H, Kolterman B E, Lansdell C P, Linnemann J T, McEnery J E, Mincer A I, Nemethy P, Noyes D, Pretz J, Ryan J M, Parkinson P M S, Shoup A, Sinnis G, Smith A J, Sullivan G W, Vasileiou V, Walker G P, Williams D A and Yodh G B 2008 *Physical Review Letters* **101** 221101 (*Preprint* `0801.3827`)

[16] Bzowski M, Kubiak M A, Moebius E, Bochsler P, Leonard T, Heirtzler D, Kucharek H, Sokol J M, Hlond M, Crew G B, Schwadron N A, Fuselier S and McComas D J 2012 *Astrophys. J. Suppl.* **In Press**

[17] Amenomori M, Bi X J, Chen D, Cui S W, Danzengluobu, Ding L K, Ding X H, Fan C, Feng C F, Feng Z, Feng Z Y, Gao X Y, Geng Q X, Guo H W, He H H, He M, Hibino K, Hotta N, Hu H, Hu H B, Huang J, Huang Q, Jia H Y, Kajino F, Kasahara K, Katayose Y, Kato C, Kawata K, Labaciren, Le G M, Li A F, Li J Y, Lou Y Q, Lu H, Lu S L, Meng X R, Mizutani K, Mu J, Munakata K, Nagai A, Nanjo H, Nishizawa M, Ohnishi M, Ohta I, Onuma H, Ouchi T, Ozawa S, Ren J R, Saito T, Saito T Y, Sakata M, Sako T K, Shibata M, Shiomi A, Shirai T, Sugimoto H, Takita M, Tan Y H, Tateyama N, Torii S, Tsuchiya H, Udo S, Wang B, Wang H, Wang X, Wang Y, Wang Y G, Wu H R, Xue L, Yamamoto

Y, Yan C T, Yang X C, Yasue S, Ye Z H, Yu G C, Yuan A F, Yuda T, Zhang H M, Zhang J L, Zhang N J, Zhang X Y, Zhang Y, Yizhang, Zhaxisangzhu, Zhou X X and The Tibet ASγ Collaboration 2011 *Proc. of 32nd ICRC* (Beijing, China) p paper 0379

[18] Frisch P C, Redfield S and Slavin J D 2011 *Ann. Rev. Astron. Astrophys.* **49** 237–279

[19] Frisch P C, Grodnicki L and Welty D E 2002 *Astrophys. J.* **574** 834–846

[20] Wood B E, Linsky J L and Zank G P 2000 *Astrophys. J.* **537** 304–311

[21] Frisch P C and Mueller H R 2011 *Space Sci. Rev.* 130 (*Preprint* 1010.4507)

[22] Lallement R, Bertin P, Ferlet R, Vidal-Madjar A and Bertaux J L 1994 *Astron. Astrophys.* **286** 898–908

[23] Hébrard G, Mallouris C, Ferlet R, Koester D, Lemoine M, Vidal-Madjar A and York D 1999 *Astron. Astrophys.* **350** 643–658 (*Preprint* arXiv:astro-ph/9909061)

[24] Linsky J L, Rickett B J and Redfield S 2008 *Astrophys. J.* **675** 413–419

[25] Redfield S and Linsky J L 2008 *Astrophys. J.* **673** 283–314 (*Preprint* arXiv:0709.4480)

[26] Smirnova T V, Gwinn C R and Shishov V I 2006 *Astron. Astrophys.* **453** 601–607 (*Preprint* arXiv:astro-ph/0603490)

[27] Bzowski M, Kubiak M A, Möbius E, Bochsler P, Leonard T, Heirtzler D, Kucharek H, Sokół J M, Hłond M, Crew G B, Schwadron N A, Fuselier S A and McComas D J 2012 *Astrophys. J. Suppl.* **198** 12 (*Preprint* 1202.0415)

[28] Möbius E, Bochsler P, Bzowski M, Heirtzler D, Kubiak M A, Kucharek H, Lee M A, Leonard T, Schwadron N A, Wu X, Fuselier S A, Crew G, McComas D J, Petersen L, Saul L, Valovcin D, Vanderspek R and Wurz P 2012 *Astrophys. J. Suppl.* **198** 11

[29] Wolleben M 2007 *Astrophys. J.* **664** 349

[30] Schwadron N A, Allegrini F, Bzowski M, Christian E R, Crew G B, Dayeh M, DeMajistre R, Frisch P, Funsten H O, Fuselier S A, Goodrich K, Gruntman M, Janzen P, Kucharek H, Livadiotis G, McComas D J, Moebius E, Prested C, Reisenfeld D, Reno M, Roelof E, Siegel J and Vanderspek R 2011 *Astrophys. J.* **731** 56

[31] Schönrich R, Binney J and Dehnen W 2010 *MNRS* **403** 1829–1833 (*Preprint* 0912.3693)

[32] Shalchi A, Büsching I, Lazarian A and Schlickeiser R 2010 *Astrophys. J.* **725** 2117–2127